

Mid-Atomic-Number Cylindrical Wire Array Precursor Plasma Studies on Zebra

A. Stafford^a, A.S. Safronova^a, V.L. Kantsyrev^a, M.E. Weller^a, I. Shrestha^a, V.V. Shlyaptseva^a, C.A. Coverdale^b, A.S. Chuvatin^c

^a*University of Nevada, Reno, NV 89557, USA*

^b*Sandia National Laboratories, Albuquerque, New Mexico 87185, USA*

^c*Ecole Polytechnique, 91128 Palaiseau, France*

Abstract – Precursor plasmas from low wire number cylindrical wire arrays (CWA) were previously shown to radiate at temperatures >300 eV for Ni-60 (96% Cu, 4% Ni) wires in experiments on the 1 MA Zebra Generator. Continued research into precursor plasmas has studied additional mid-atomic-number materials including Cu, Alumel (95% Ni, 2% Al, 2% Si) and brass (70% Cu, 30% Zn) to show the >300 eV temperatures are common for mid-atomic-number materials. Additionally current scaling effects were observed by performing CWA precursor experiments at increased current of 1.5 MA using a Load Current Multiplier (LCM). Results show an increase of linear radiation yield of $\sim 50\%$ (16 kJ/cm vs. 10 kJ/cm) for the experiments at increased current. However, plasma conditions inferred through the modeling of x-ray time gated spectra are very similar for the precursor plasma in both current conditions.

I. INTRODUCTION

Z-pinches are efficient x-ray generators and have therefore been studied for knowledge useful for many disciplines including: high energy density physics [1], inertial confinement fusion [2], and astrophysics [3]. Precursor plasmas from cylindrical wire array (CWA) Z-pinches have been studied for their role in wire implosion dynamics and their potential to preheat a target for inertial confinement fusion [4]. Precursor plasmas have been studied on many machines but in the most detail using MAGPIE [5-7]. MAGPIE is a ~ 1 MA machine with a 240 ns rise time. The MAGPIE experiments studied a wide range of materials from Al to W. Electron temperatures for Al precursor columns were inferred to be ~ 50 -60 eV using radially resolved extreme ultraviolet spectra [5,7], however electron temperatures for higher atomic number materials were not estimated. Precursor plasmas from low wire number Ni-60 (96% Cu, 4% Ni) CWA Z-pinches on the 1 MA Zebra Generator were shown to have electron temperatures >300 eV [8].

This paper reports the results from continued research of precursor plasma radiation. This research studies precursor columns from CWA using additional wire materials primarily composed of mid-Z elements (Cu, Zn, and Ni) to show a consistent trend of >300 eV

electron temperatures. Additionally the current is increased to 1.5 MA to show current scaling effects of the precursor plasma conditions.

II. EXPERIMENTAL DETAILS

CWA precursor experiments were performed on the Zebra Generator at the Nevada Terawatt Facility (NTF) of the University of Nevada, Reno (UNR). The Zebra generator is a pulsed power machine capable of creating 1 MA of current with a 100 ns rise time [9]. Additionally a Load Current Multiplier (LCM) can be attached to increase the current to 1.5-1.7 MA [10]. The Zebra generator was used to implode 6 wires evenly distributed in a cylindrical pattern with a 12 mm diameter. The wires ranged between 10-15 μ m diameters and were primarily composed of mid-Z materials: 10 μ m Cu, 10 μ m Brass (70% Cu and 30% Zn), 10 μ m Alumel (95% Ni), for 1 MA and 15 μ m Ni-60 (96% Cu) for 1.5 MA experiments. Experiments performed using the standard 1 MA current had a 2 cm anode to cathode gap while the experiments using the enhanced current of 1.5 MA had a 1 cm anode to cathode gap. A full set of diagnostics were applied to each shot. The important diagnostics that will be shown are an 8 μ m Be filtered (>750 eV) photo conducting diode (PCD), a bare Ni bolometer (10 eV to 4-5 keV), x-ray time gated pinholes (>1 keV), and x-ray time gated spectra.

III. Cu CWA AT 1 MA CURRENT

The first experiment performed was a Cu CWA. This experiment produced a total radiation yield of 20 kJ as measured by a bolometer. This is a 10 kJ/cm energy output when normalized to the 2 cm anode to cathode gap. Figure 1a shows PCD and current signals for the 1 MA Cu CWA. The PCD signals record intensity of radiation for energies >750 eV. The total energy measured by the PCD was 470 J. The energy is estimated by integrating the PCD signal from first rise of the signal to when the signal returns to noise. The integrated value is then multiplied by a calibration constant for the diode. The portion due to the precursor was 14 J or 3%, calculated from first rise in signal for the precursor to the

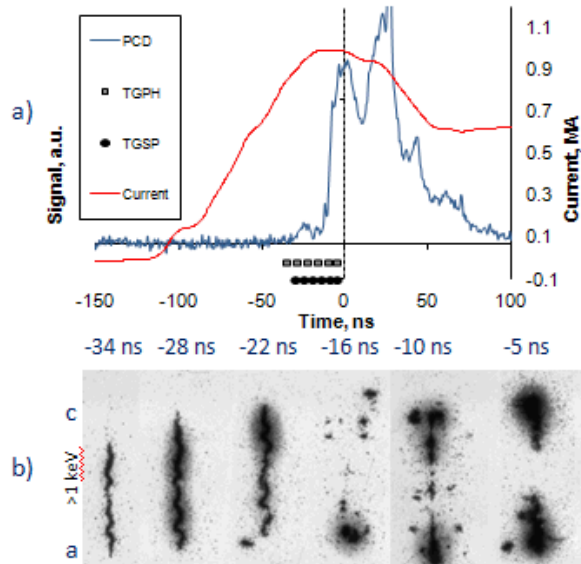


Figure 1. a) Signals for 1 MA Cu CWA including: current, PCD, x-ray time gated pinholes (TGPH), and x-ray time gated spectra (TGSP). b) X-ray time gated pinhole images for energies $>1\text{keV}$. Times are relative to the first PCD peak from main x-ray burst. Anode to cathode gap is 2 cm.

end of the drop in signal for the precursor. The PCD signals show a small peak (4 ns full width at half max, FWHM) at about -20 ns that increases and decreases before a much more intense peak which is the reference point of the graph. The small peak is due to radiation from the precursor, confirmed by the x-ray pinhole images, while the high intensity peaks that follow are from the implosion of the wires. Timings for x-ray time gated pinholes and spectra are displayed. The x-ray time gated pinholes and spectra were set to trigger during the precursor peak and lead into the wire implosion. Figure 1b shows the x-ray time gated pinhole images for $>1\text{keV}$ energies and the time relative to the first PCD peak from the wire implosion. The first pinhole image, which occurs approximately at -34 ns, shows a thin precursor plasma, estimated diameter of 1 mm, with pronounced Rayleigh-Taylor instabilities. This column grows in intensity adding a less intense cloud around the column, drops in intensity, and then breaks up around -16 ns. A new column begins to form at -10 ns and becomes an intense column at -5 ns. The clear portion in the middle of the last pinhole is due to a defect in the MCP.

Figure 2 displays the x-ray time gated spectra with timings. The x-ray time gated spectra start at -29 ns with only small signs of L-shell Cu radiation. The next frame shows prominent L-shell Cu radiation which increases in the following frame and then disappears after. In the final two frames, the L-shell Cu returns with increasing intensity and strong background radiation as the wires reach the center. Lineouts were taken for each frame during the precursor phase and modeled using a non-local thermodynamic equilibrium (non-LTE) kinetic model. The Cu model focuses on L-shell transitions and

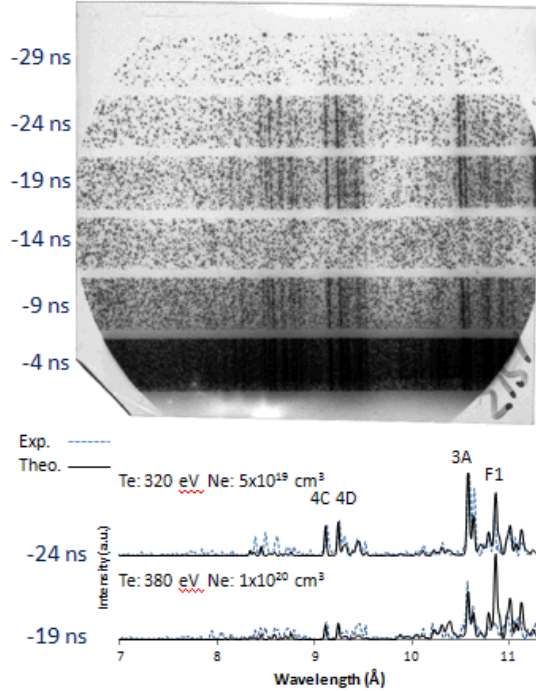


Figure 2. X-ray time gated spectra for Cu CWA. Times for spectra are relative to the first PCD from the main x-ray burst. Spectra from precursor radiation are shown compared to modeling from a Cu non-LTE kinetic model.

is described by *Ouart et al.* in reference 11. The model parameters were chosen by matching the intensity of the 4C and 4D (4-2 Ne-like transitions) lines for scaling. Then the electron density parameter was adjusted to match the 3A (3-2 Ne-like transition) line, while the electron temperature was adjusted to match the F-like (3-2 F-like transitions) lines on the high wavelength side of the 3A transition. The modeling suggests electron temperatures starting at 320 eV for the first precursor spectrum and rising to 380 eV for the last precursor spectrum before the L-shell Cu disappears. The electron density starts at $5 \times 10^{19} \text{ cm}^{-3}$ and rises to $1 \times 10^{20} \text{ cm}^{-3}$. This modeling suggests the higher electron temperatures for precursor plasmas from Ni-60 CWAs are also found for pure Cu CWAs.

IV. ALUMEL CWA AT 1 MA CURRENT

Alumel is a Ni alloy with 95% Ni, 2% Al, and 2% Si. Alumel CWA experiments were performed for comparison with other mid-Z materials and a typical example is shown. The total radiation yield for the Alumel CWA experiment was 17 kJ or 8.5 kJ/cm. The PCD and current signals for the Alumel CWA experiment can be seen in Figure 3a. Alumel CWAs show much more prominent precursor radiation (11 ns FWHM) relative to the main implosion. In the PCD signal, the strong precursor radiation peaks at approximately -35 ns and decreases before the main

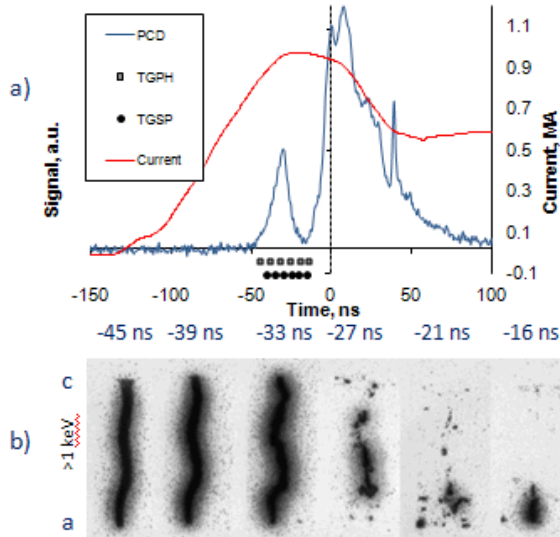


Figure 3. a) Signals for 1 MA Alumel CWA including: current, PCD, x-ray time gated pinholes (TGPH), and x-ray time gated spectra (TGSP). b) X-ray time gated pinhole images for energies $>1\text{keV}$. Times are relative to the first PCD peak from main x-ray burst. Anode to cathode gap is 2 cm.

implosion which first peaks at the origin. The total energy measured by the PCD was 566 J. The precursor provided 70 J or 12%. The x-ray time gated pinholes and spectra were triggered to start in the early stages of the precursor and record the evolution of the plasma until the beginning of the PCD signal rise due to the main implosion. Figure 3b shows the x-ray time gated pinhole images with their timings. The pinhole images start with a high intensity column at -45 ns that grows more intense until -33 ns. Estimates of the size of the high intensity region of the column suggest a diameter as big as 1.5 mm. The column is around 50% thicker for the Alumel experiment than the Cu experiment and the instabilities of the Alumel precursor have a longer wavelength. After -33 ns the column starts dispersing before the intensity begins to increase with the onset of the main implosion. As with the Cu CWA experiment the last frame of the pinhole image is affected by a defect of the MCP in the middle.

In Figure 4, the x-ray time gated spectra start in the early stages of precursor radiation as seen in the PCD signal and end at the beginning of the PCD signal rise due to the main implosion. The spectra show an increase and fade in intensity that correlates with the PCD signal. Non-LTE kinetic modeling of the L-shell Ni indicates an electron temperature of $\sim 400\text{ eV}$ for the earliest timing (-41 ns). The electron temperature then decreases to about 340 eV (-21 ns) before increasing to about 390 eV (-16 ns). The density was kept constant at $5 \times 10^{19}\text{ cm}^{-3}$ which is a common electron density for Z-pinch plasmas. This was done because there were not good density diagnostic lines in the spectral region available. The electron temperature was determined by matching the line

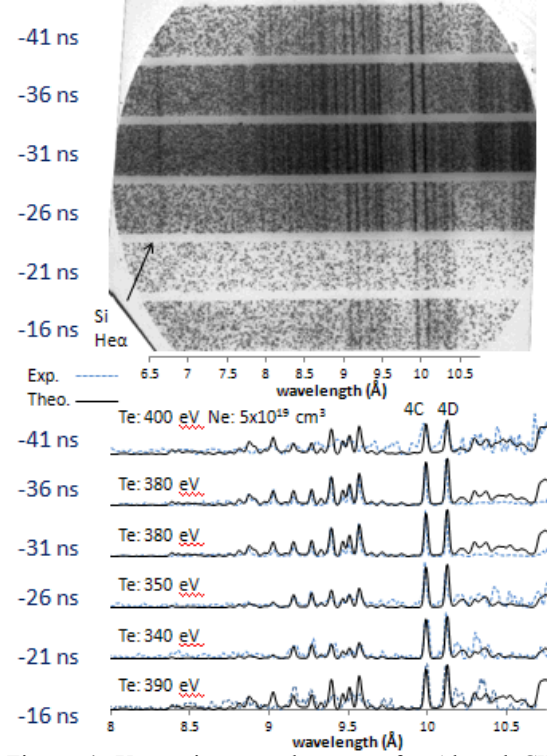


Figure 4. X-ray time gated spectra for Alumel CWA. Times for spectra are relative to the first PCD from the main x-ray burst. Spectra from precursor radiation are shown compared to modeling from a Ni non-LTE kinetic model. All modeling used $\text{Ne: } 5 \times 10^{19}\text{ cm}^{-3}$.

structures surrounding the 4C and 4D transition lines. Again $>300\text{ eV}$ temperatures are observed for a mid-Z material.

V. Ni-60 CWA AT 1.5 MA CURRENT

Ni-60 (96% Cu, 4% Ni) CWA experiments were performed with the addition of the LCM to test the current scaling effect on the precursor plasma. The LCM experiments require reducing the anode to cathode gap to 1 cm. The Ni-60 CWA experiments have a total radiation yield of $\sim 16\text{ kJ}$ or 16 kJ/cm for comparison with the 1 MA experiments. The PCD and current signals for a typical experiment can be seen in Figure 5a. A strong precursor bump (8 ns FWHM) similar to the Alumel CWA is seen in the PCD signals and peaks around -30 ns. The total energy measured by the PCD was 750 J. The precursor radiation accounted for 40 J or 5%. The signals also display the x-ray time gated pinholes and spectra timings which begin in the precursor radiation bump and end early into the radiation rise of the main implosion. The x-ray time gated pinhole images are shown in Figure 5b. The pinholes recorded 2 frames of strong radiation from a column, estimated diameter of approximately 1.5 mm, followed by two frames of scattered small radiation spots which again return to strong radiation from a column along with scattered spots of radiation. This shows the change from precursor

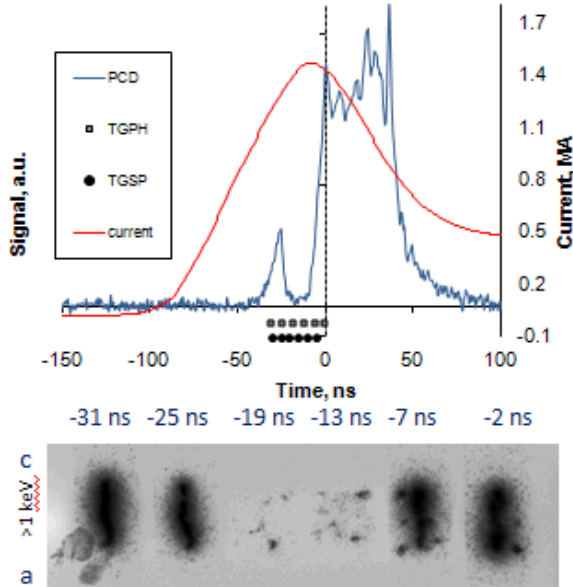


Figure 5. a) Signals for 1.5 MA Ni-60 CWA including: current, PCD, x-ray time gated pinholes (TGPH), and x-ray time gated spectra (TGSP). b) X-ray time gated pinhole images for energies $>1\text{keV}$. Times are relative to the first PCD peak from main x-ray burst. Anode to cathode gap is 1 cm.

radiation to the beginning of the main implosion radiation.

In Figure 6, the x-ray time gated spectra start near the peak of the precursor plasma radiation. The intensity of the spectra decreases with the fall in radiation and mostly disappears by the fourth frame. This continues until the end when the spectrum returns with the rise of the radiation from the main implosion. Modeling of L-shell Cu was matched to the three frames connected to the precursor plasma. The modeling suggests electron temperatures starting at approximately 390 eV which drops to 310 eV in the next frame. The last precursor spectrum shows a rise in temperature to 330 eV. The electron density follows a reverse trend starting at $5 \times 10^{19} \text{ cm}^{-3}$ and increasing to $9 \times 10^{19} \text{ cm}^{-3}$ before dropping to $1 \times 10^{19} \text{ cm}^{-3}$.

VI. CONCLUSIONS

The recent experiments of mid-atomic-number CWAs have shown a consistent trend of >300 eV temperatures for the precursor plasma. X-ray time gated pinhole images were able to record the full evolution of the precursor plasma for Cu and Alumel CWAs. The pinhole images recorded the instabilities of the columns and a correlation of intensity with peaks in the PCD signal. Estimates of the size of the precursor column suggest diameters around 1 mm for the Cu CWA and 1.5 mm for the Alumel CWA. The pinhole images also show radiating mass surrounding the intense precursor column that varies with material and current. The Cu CWA

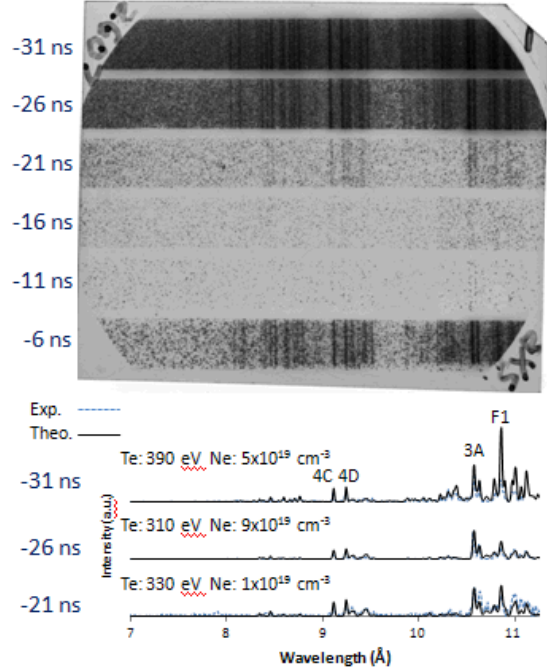


Figure 6. X-ray time gated spectra for Ni-60 CWA. Times for spectra are relative to the first PCD from the main x-ray burst. Spectra from precursor radiation are shown compared to modeling from a Cu non-LTE kinetic model.

precursor plasma has very little radiation outside the intense column, while the Alumel CWA has a consistent cloud of radiating mass. The PCD signal indicates significant material dependence for radiation intensity from precursor plasmas that correlates with the results from the pinhole images. The Cu CWA precursor plasma amounted to 3% of the total radiation in the PCD regime, while the Alumel CWA precursor plasma accounted for 12%. The material also affected the duration of the precursor radiation. The Cu CWA was the shortest precursor with a 4 ns FWHM and the longest precursor was from the Alumel CWA with an 11 ns FWHM. The modeling suggests the Alumel precursor plasma had temperatures slightly higher than the Cu precursor plasma and they lasted for a longer duration. Combining all these results, The Alumel CWA was the best precursor radiator.

The best comparison for determining the effects of current scaling is the Cu CWA experiment performed at 1 MA and the Ni-60 CWA experiment performed at 1.5 MA. The time gated pinhole images recorded most of the evolution of the Ni-60 precursor plasma. The Ni-60 precursor plasma shows a thicker intense column with a diameter of approximately 1.5 mm compared to the 1 mm Cu precursor column. Additionally the Ni-60 precursor plasma had a very intense cloud of radiating mass surrounding the column compared to very little radiating mass for the Cu precursor plasma. This is in agreement with the energies measured by the PCD. The radiated energy of the Ni-60 precursor plasma in the PCD regime was 40 J compared to 14 J for the Cu

precursor plasma. Modeling of the time gated spectra suggests conditions for the Ni-60 precursor plasma were very similar to the Cu precursor plasma. With these results, the increased current of 1.5 MA created a larger precursor plasma that radiated more energy due to more mass in similar conditions to the 1 MA precursor plasma.

Future work will look into alternate arrays of mixed mid-Z wires and Al wires to study the effects of non-uniformity on precursor plasmas. The focus will be looking for high temperature Al in the precursor column due to warming from the mid-Z material as well as comparing the precursor properties to both uniform mid-Z and Al CWAs.

ACKNOWLEDGMENTS

This work was supported by NNSA under DOE Coop. Agr. DE-NA0001984 and in part by DE-FC52-06NA27616. Sandia National Laboratories is a multi-program laboratory managed and operated by Sandia Corporation, a wholly owned subsidiary of Lockheed Martin Company, for the U.S. Department of Energy's National Nuclear Security Administration under Contract DE-AC04-94AL85000.

We would like to thank all Nevada Terawatt Facility staff that helped in attaining experimental data. We would also like to thank former UNR team members Dr. N.D. Ouart, Dr. K.M. Williamson, and Dr. G.C. Osborn for their contributions.

REFERENCES

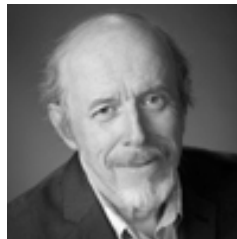
- [1] M. K. Matzen *et al.*, Phys. Plasmas **12**, 055 503 (2005).
- [2] M. E. Cuneo *et al.*, Phys. Plasmas **13**, 056 318 (2006).
- [3] S.V. Lebedev *et al.*, Plasma Phys. Controlled Fusion **47**, B465 (2005).
- [4] S. C. Bott *et al.*, Rev. Sci. Instrum. **75**, 3944 (2004).
- [5] S. C. Bott *et al.*, Phys. Rev. E **74**, 046403 (2006).
- [6] S.V. Lebedev *et al.*, Laser Part. Beams **19**, 355 (2001).
- [7] F. N. Beg *et al.*, IEEE Trans. Plasma Sci. **30**, 552 (2002).
- [8] C.A. Coverdale *et al.*, PRL **102**, 155006 (2009).
- [9] D. J. Ampleford *et al.*, Phys. Plasmas **14**, 102 704 (2007).
- [10] A.S. Chuvatin *et al.*, Physical Review, S.T. Accelerators and Beams **13**, 010401 (2010).
- [11] N.D. Ouart *et al.*, 4th Special Issue of the IEEE Transaction on Plasma Science on Z-pinch Plasma **38**, 631 (2010).



Austin Stafford was born in Upland, CA, on August 15, 1987. He received the B.S. degree in physics and mathematics from Linfield College, McMinnville, Oregon, in 2009. He is currently working toward the Ph.D. degree at the University of Nevada, Reno where he is involved in theoretical work on X-ray spectroscopy of Z-pinch.



Alla S. Safronova (M'06) was born in Moscow, Russia. She received a Ph.D. degree in physics from the Institute of General Physics, Russian Academy of Science (RAS), Moscow, in 1986. From 1994 to 1998, she was first a Visiting Scientist and then a Postdoctoral Research Associate with the Department of Physics, University of Nevada, Reno, where since 1998 she has been an Associate Research Professor and is now a Research Professor. Her former PhD students are working in Sandia National Laboratories, Naval Research Laboratory, and also abroad at various universities. She is one of the pioneers in the application of X-ray line polarization to astrophysical and laboratory plasmas. Her current research includes studying of radiation from and processes in High Energy Density plasmas such as Z-pinch and high-power laser plasmas, and tokamak plasmas. She organized and chaired the series of international workshops on Radiation from High Energy Density Plasmas (RHEDP 2011 and 2013) as well as sessions at ICOPS and other international meetings on plasma physics, and was the guest editor of 5th Special Issue of IEEE TPS on Z-pinch Plasmas (2012) and of the special topic section on RHEDP of Physics of Plasmas (2014).



Victor L. Kantsev (M'06) received the M.S. and Ph.D. degrees from Moscow Engineering Physics Institute, in 1972 and 1981, respectively, and has the advanced degree of Dr. Sci. (equivalent of the Dr. Habil. degree in Europe) from the Institute of Analytical Instrumentation (St. Petersburg, Russia) Russian Academy of Science in 1992. From 1972 to 1995, he has been a Researcher, Head of a Sector, and Head of Laboratory in several Russian scientific research institutes in Moscow. From 1982 to 1994 he has also been part time Docent (equivalent of the Associate Professor in the USA) in Moscow Institute

of Radio-Engineering, Electronics and Automation. In 1994, he was a Visiting Scholar and Lecturer with the Department of Physics, University of Nevada, Reno, where he has been a Research Professor since 1996. Prof. Kantsyrev has supervised 5 graduated Ph.D. and 11 M.S. students. His current research interests include high energy density physics and pulsed power, such as radiative properties and implosion dynamics of different wire-arrays and X-pinch plasmas and their applications for radiation physics and inertial confinement fusion, interaction of ultrashort laser pulse with matter and plasma diagnostics. He organized and chaired technical areas and sessions at several International Conferences.

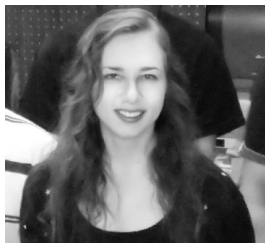


Michael E. Weller (M'14) was born in Visalia, CA, on November 4, 1984. He received a B.S. degree in physics from Arkansas Tech University, Russellville, AR in 2007. He interned at the University of Arkansas, Fayetteville, where he worked in the nanotechnology field, in the summer of 2006. He also

interned at the JPL, Pasadena, California, where he worked in the atmospheric field, in the summer of 2007. He received his Ph.D. in physics from the University of Nevada, Reno in 2014, studying theoretical and experimental physics related to z-pinches. He is currently working at the University of Nevada, Reno as a Postdoctoral Scholar where he continues his work in physics related to z-pinches.



Ishor Shrestha was born in Gorkha, Nepal. He received the M.S. degree from Tribhuvan University, Kathmandu, Nepal. He was a Lecturer in Physics at Tribhuvan University for eight years. He received the Ph.D. degree from University of Nevada Reno, USA in 2010. He is currently working as a Post-Doctoral Research Associate in the Department of Physics, University of Nevada, Reno. He has published more than 50 papers in scientific journals. His research interests include hard X-ray polarimetry diagnostic development, laser plasma, wire arrays and x-pinch research.



Veronica Shlyaptseva (M'12) was born in Moscow, Russia in 1984. She received her B.A. from the University of Nevada, Reno in 2008 where she is currently a staff member. She is working on x-ray

diagnostics and spectroscopy of Z-pinch and laser plasmas and on modeling of hohlraum experiments.